Bundesanstalt für Materialforschung und -prüfung

Certification Report

Certified reference material for surface analysis

BAM-L200

Nanoscale stripe pattern for testing of lateral resolution and calibration of length scale

M. Senoner

Bundesanstalt für Materialforschung und –prüfung (BAM)

D-12200 Berlin, Germany

Contents

	page
Abbreviations	2
1. Introduction	3
2. Selection of material	4
3. Preparation of the sample	4
4. Certification	5
4.1. Procedures and certification strategy	5
4.2. Determination of certified values from TEM measurements	6
4.3. Determination of certified values from SEM measurements	8
4.4. Calculation of uncertainties	10
4.4.1. Sources of uncertainty and their contribution to combined uncertainty	10
4.4.1.1. TEM	10
4.4.1.2. SEM	12
4.4.2. Calculation of combined uncertainty	12
4.4.2.1. TEM	12
4.4.2.2. SEM	12
5. Homogeneity of samples	15
5.1. Homogeneity of layer thickness over the wafer	15
5.1.1. X-ray diffraction	15
5.1.2. Optical reflection spectroscopy	18
5.1.3. TEM measurements	21
5.1.4. Definition of useful area	21
5.2. Wafer-to-wafer homogeneity	21
6. Stability of samples	22
7. Fields of Application	22
8. Instruction for users	23
9. References	23
Appendix: Image numbers of TEM images (sheet films)	24

Abbreviations

AES	Auger Electron Spectroscopy
CRM	Certified Reference Material
DBR	Distributed Bragg Reflector
ESF	Edge Spread Function
ESCA	Electron Spectroscopy for Chemical Analysis
FIB	Focused Ion Beam
HRXRD	High Resolution X-ray Diffraction
LSF	Line Spread Function
MOVPE	Metal Organic Vapor Phase Epitaxy
MTF	Modulation Transfer Function
PTB	Physikalisch-Technische Bundesanstalt
SD	Standard Deviation
SEM	Scanning Electron Microscope
SIMS	Secondary Ion Mass Spectrometry
TEM	Transmission Electron Microscope

1. Introduction

The progress of nanotechnology and its future demands are driving the improvement of surface analysis and imaging in the nanometer range. The performance of the applied methods is substantially determined by their lateral resolution and the permanent control of lateral resolution is an important part of quality assurance in surface analysis. As a consequence, appropriate test samples for the determination of lateral resolution are needed.

The analysis of lateral resolution in the range between the dimensions of the crystal lattice (< 1 nm) and lithographic patterns (> 30 nm) was limited to the analysis of sharp edges (step transitions), because no other regular patterns in this region were available. The first attempt to overcome this situation was the development of the certified reference material BAM-L002. This CRM was introduced in 2003 and successfully applied in an inter-laboratory comparison concerning the lateral resolution of SIMS [1]. BAM-L002 is a cross section of a semiconductor layer stack. The surface of the sample provides a flat pattern with strip widths ranging from 1 to 500 nm and two square-wave gratings with different periods [2]. The restriction to two gratings in the pattern does not allow the estimation of lateral resolution and the determination of the modulation transfer function (MTF).

To overcome this disadvantage BAM has developed the new reference material BAM-L200. It is a cross section of an AlGaAs - InGaAs - GaAs layer stack and 142 layers yield a complex strip pattern in the surface of the sample (see fig.1). 23 gratings with finely graded periods between 2 nm and 600 nm enable the real time estimation of lateral resolution and the determination of MTF. Furthermore narrow stripes between 1 nm and 40 nm enable the determination of the line spread function (LSF) and step transitions enable the determination of the edge spread function (ESF), which also characterizes the lateral resolution.

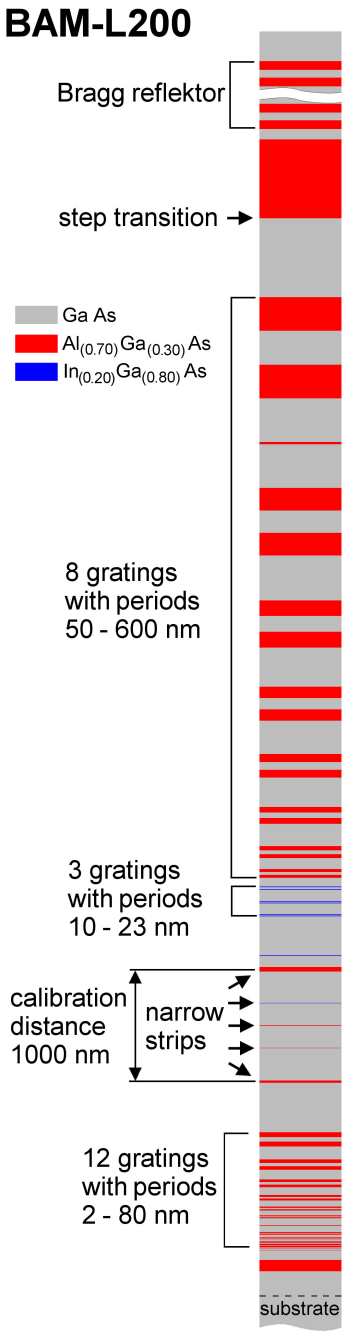

Fig. 1: Scheme of stripe pattern on the surface of BAM-L200

2. Selection of material

The selection of materials was based on two criteria:

1. Layers with sharp interfaces and constant thicknesses between 1 nm and 700 nm may be produced by a well proven technology.
2. The material contrast must be sufficient for imaging of the stripes in the surface of the sample with the most important methods of surface analysis.

The best method to prepare high quality layers with sharp interfaces is epitaxial growth. Therefore we looked for a suitable system of semiconductor heterojunctions. Multilayer systems of AlGaAs and GaAs are well known in optoelectronics and their preparation with MOVPE is a well proven technology. Due to the good fit of the lattice constants of GaAs and AlAs it is possible to prepare thick layers (several hundreds of nanometers) with a great difference in elemental composition. For this reason we used the system GaAs – $Al_{0.7}Ga_{0.3}As$. Additionally some thin layers of $In_{0.2}Ga_{0.8}As$ are included in the layer stack. The partial substitution of Ga by Al gives a sufficient material contrast for all tested methods of surface analysis (see section 7).

3. Preparation of the sample

The multilayer structure was grown by Metal Organic Vapor Phase Epitaxy (MOVPE) at the Ferdinand-Braun-Institut für Höchstfrequenztechnik. The layer stack has a total thickness of about 12 µm. A batch of 5 wafers with a diameter of 4 inches was coated during one continuous procedure.

The coated wafer was sawed into small platelets of 3.2 mm × 2.7 mm. They were coated with Ti, Au, Cr and Cu and each platelet was mounted in a clamp of nonmagnetic stainless steel (Fig. 2).

A milled hole on the stainless steel area serves as a marker for the side of the platelet which is coated by the layer stack. Grinding and polishing of the sample surface produces a flat cross section with a roughness of about 1-2 nm. However, the sample surface may show a few scratches. Areas affected by scratches should not be used for imaging. The surface of the multilayer stack is displayed as a stripe pattern (Fig. 5).

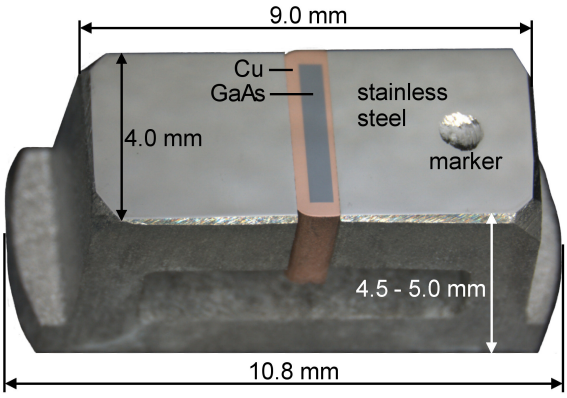

Fig. 2: Sample

4. Certification

4.1. Procedures and certification strategy

The certified values (red lettering in Fig. 3) are stripe widths W, grating periods P of square-wave gratings (twice the stripe width W) and stripe distances D. The stripe distances are center-to-center distances between narrow stripes and/or fine 3-stripe gratings, respectively. This definition of distance does not depend on lateral resolution of the image. Furthermore this definition enables the addition of neighboring certified distances, e.g. D1 + D2 (cf. Fig. 3).

$In_{0.2}Ga_{0.8}As$ stripes (5 nm) and $Al_{0.7}Ga_{0.3}As$ stripes with widths smaller than 3.5 nm were not certified because the quality of images was not sufficient for the determination of such small strip widths. Furthermore the $In_{0.2}Ga_{0.8}As$ layers W13 and P21 – P23 may show variations in layer thickness due to the formation of quantum dots. The corresponding characteristics (black italic lettering in Fig.3) are non-certified values declared by the manufacturer.

The imaging method with the highest lateral resolution, maximum sharpness of the images and correspondingly maximum accuracy in length measurement is the Transmission Electron Microscopy (TEM). Therefore we used this method to determine the certified values.

The calibration of length scale of the TEM is based, via an intermediate standard (see 4.2.), on the lattice constant of silicon which is traced back to definition of the meter. Corresponding measurement with a calibrated TEM ensures an unbroken chain of traceability from the measured length to the definition of the meter.

Due to the high constancy of layer thickness it is possible to certify the whole batch of 5 wafers by a limited number of TEM measurements. The analysis of homogeneity (see section 5) ensures that the certified values are valid for all samples made from this batch.

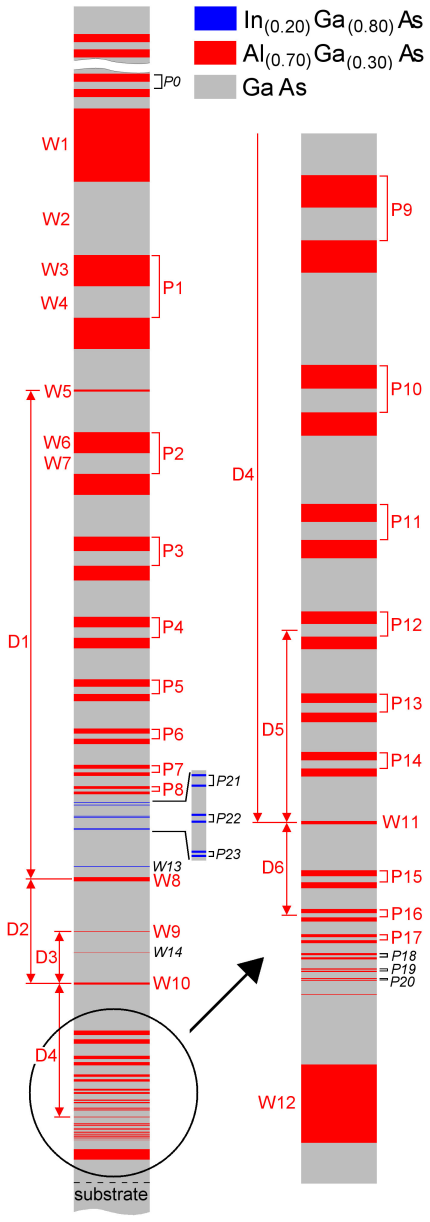

Fig. 3: Certified (red lettering)and non-certified (black italic lettering) characteristics.

For measurements of longer distances ($D \geq 1$ µm) TEM measurements were complemented by the use of Scanning Electron Microscopy (SEM). SEM images enable a high accuracy determination of distances at magnifications below 50 000, especially between narrow lines (Fig. 5). The uncertainty of values is reduced by SEM measurements because the length scale of the SEM instrument was calibrated with a standard having smaller uncertainties for distances longer than 1 µm compared to the standard for calibrating the TEM length scale.

Furthermore SEM measurements are particularly suitable for quality control and tests of sample homogeneity because they may be performed at readily prepared samples, whereas TEM measurements demand the very time-consuming preparation of thin lamellae.

4.2. Determination of certified values from TEM measurements

The preparation of TEM-lamellae by focused ion beam (FIB) milling and TEM measurements were done at BAM division V.1. The determination of certified values is based on the evaluation of 5 TEM-lamellae taken from the central part of the wafer (5 mm from center) and 2 TEM-lamellae taken from the boundary of the used wafer area (30 mm from center), respectively. From these lamellae more than 100 images were taken at different magnifications between 10 000 and 300 000.

TEM measurements were performed using a JEOL 4000FX Microscope at an operating voltage of 400 kV. TEM images were recorded on sheet film. The magnification of the TEM instrument was calibrated by means of a certified magnification calibration sample (MAG*I*KAL™ from Norrox Scientific, Canada). This standard was calibrated by the manufacturer with respect to the (111) lattice spacing of silicon, which itself is traced back to definition of the meter.

The quality (sharpness) of TEM images depends on thickness and quality (bending, surface damage) of the prepared lamellae and varies in a wide range. Fig. 4 shows a selection of the best TEM images taken at different magnifications. The dark lines, e.g. in image 7471, are bend contours due to a weak bending of the TEM lamellae.

The length L measured by TEM is given by

$$L = L_F / M, \qquad (1)$$

where L_F is the length measured on sheet film and M is the real magnification of TEM taken from the linear calibration function and given in Tab. 3. The measurements of L_F were carried out using a glass scale in TEM negative images on sheet film. Tab. 1 gives values taken from more than 100 images of 7 lamellae taken from the central part of the wafer (5 mm from

center) and the boundary of the used wafer area (30 mm from center), respectively. No variation of lengths between these two positions on the wafer was observed. The certified value is the arithmetic mean of all values given in Tab. 1 and characterizes all samples taken from the wafer within a radius of 30 mm.

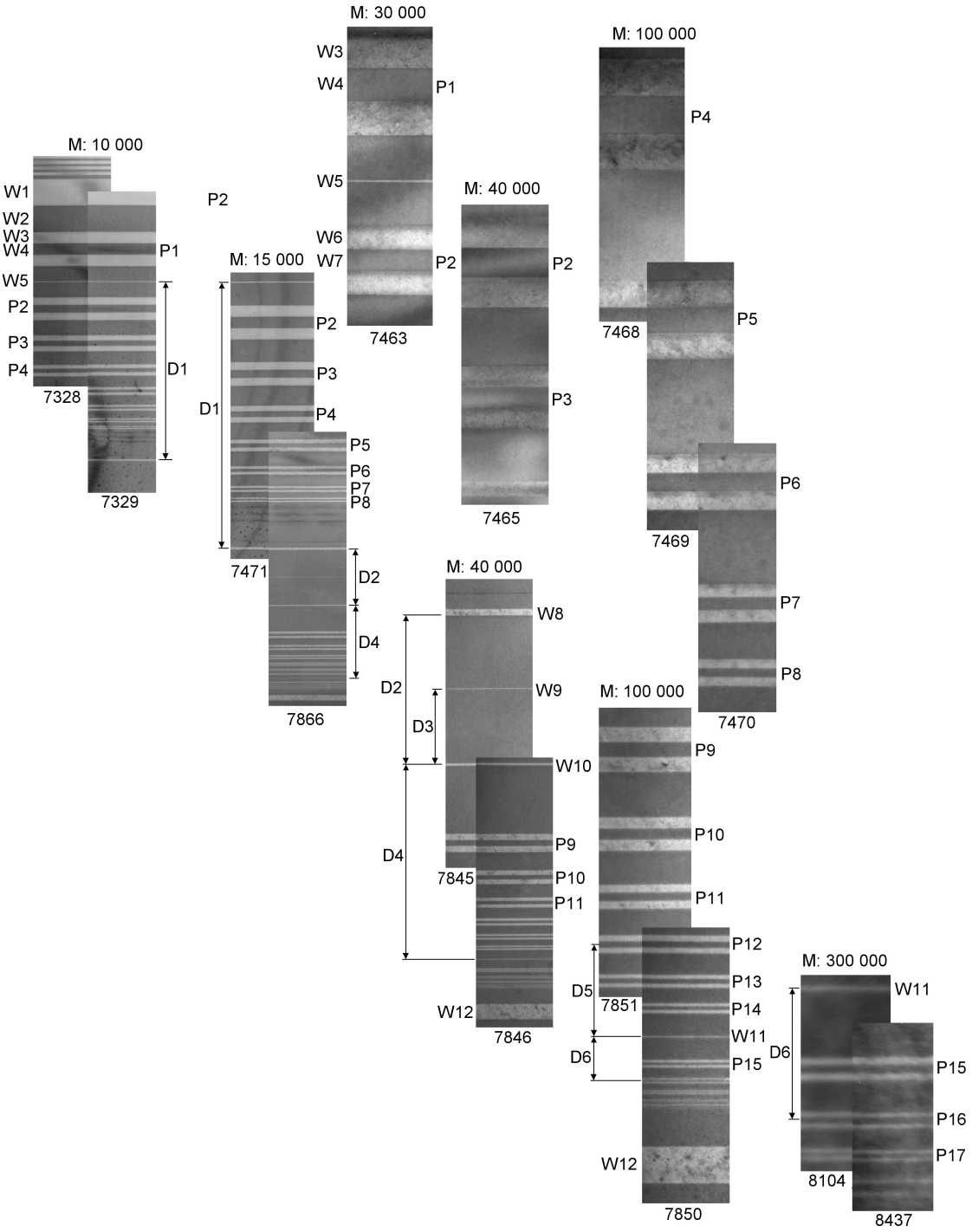

Fig. 4: Selection of TEM images taken at different magnifications M. The nominal value of M is given above the image. W, P and D designates strip widths, grating periods and distances, respectively. The number of sheet film is given below the image.

characteristic	measured values (nm)											mean	2 * standard dev.
	position 5 mm							position 30 mm					
W1	692			676	697			697				**691**	**19.9**
W2	692			676	697			697				**691**	**19.9**
W3	297	290	297	290	292	290		297				**293**	**7.1**
W4	297	290	297	290	297	290		297				**294**	**7.5**
W5		19	19			19	20.5					**19.4**	**1.5**
W6	195	191	195	196	195	195	198	195				**195**	**3.9**
W7	195	191	195	196	195	195	198	195				**195**	**3.9**
W8	38.5	38.5	37	38.5	37				38.5			**38.0**	**1.5**
W9	3.8	3.6		3.8					3.3			**3.6**	**0.5**
W10	15	15	14	14	14				13			**14.2**	**1.5**
W11	4	3.4				3.4			3.4	3.1		**3.5**	**0.7**
W12	96	95	97.5		96		96		95			**96**	**1.8**
P1	594	580	590	580	589	580		594				**587**	**13.1**
P2	394	382	392	392	387	389	390	389				**389**	**7.4**
P3	277			272	272		274	272				**273**	**4.4**
P4	195		192	192	191	196	192	195				**193**	**4.0**
P5	133			137	134	140	137	133				**136**	**5.6**
P6	95	96	97	99	96	98	96	97				**97**	**2.6**
P7		67.5	68.5	68	67	65.5	68.5					**67.5**	**2.3**
P8		49	48	50.5	47	48	48					**48.4**	**2.4**
P9	77				77	76		77	76			**76.6**	**1.1**
P10	57				58	57		57	56			**57.0**	**1.4**
P11	42				42	42		43	42			**42.2**	**0.9**
P12	31	31	31			31	31	31	31			**31.0**	**0.0**
P13	22.5	22.5	22.5			23.5	22.5	23.1	23.6			**22.9**	**1.0**
P14	17.5	16.9	17.4				17.5	17.1	18.4			**17.5**	**1.0**
P15	13.0	12.3				13.7	13.7	12.8	13.3	13.7	13.7	**13.3**	**1.1**
P16	9.5	8.2				9.5	10.2	8.5	9.2	10.2	9.5	**9.4**	**1.4**
P17	7.5					6.8	6.8			6.8	6.8	**6.9**	**0.6**
D1	4641	4662	4652	4623				4631	4641			**4642**	**28.0**
D2	990	989	977	973	986		982	994	989	987	989	**986**	**12.9**
D3	496		488	486	493		490	492	492	492	497	**492**	**7.0**
D4	1269	1265	1270		1264	1255			1260		1263	**1264**	**10.3**
D5	238	241			238	233	240			232	234	**237**	**7.1**
D6	115	115			114	113	116	114	114	114	113	**114**	**1.9**

Tab. 1: Values measured in TEM images of different magnifications. The TEM lamellae were taken 5 mm and 30 mm from the center of the wafer, respectively. The image numbers of sheet films in which the lengths were measured are given in Tab. A1 (appendix). Note that the standard deviations given in the last column are ***not*** *the uncercertainties given in the certificate (see Tab. 3).*

4.3. Determination of certified values from SEM measurements

The SEM measurement was performed using a Zeiss Gemini Supra 40 at BAM division VI.4 The length scale was calibrated by means of a silicon chip with etched groups of lines (IMS HR 98 727-04 183) certified by Physikalisch-Technische Bundesanstalt (PTB) (calibration mark 4319PTB05). The calibration measurement yields a correction factor of 1.0066, which is included in Tab. 2 but not in Fig. 5.

SEM images were taken of four readily prepared samples and the distances D1 and D2 (see Fig. 3) were measured by positioning two cursors. Cuttings from these images with the measure of D1 are shown in Fig. 5. The values for D1 and D2 are given in Tab. 2. They support the values measured by TEM and reduce their uncertainty (see 4.4.1.1.). The

certified value of D1 is taken from SEM measurements, because its uncertainty is smaller than that of TEM measurements (see 4.4.2.).

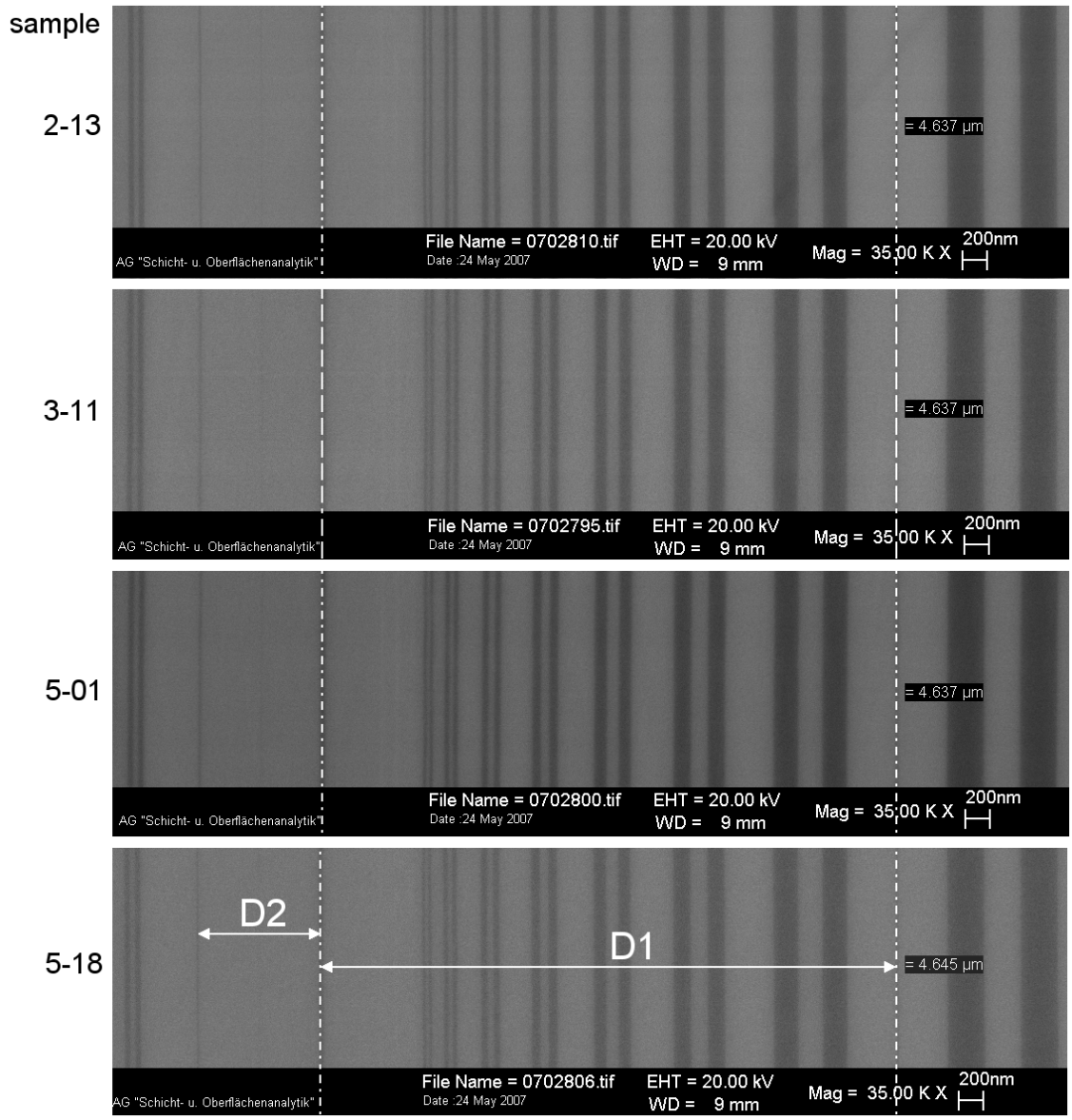

Fig. 5: SEM images taken with a Zeiss Gemini Supra 40 in the backscattered electron mode. The cursors mark the 40 nm wide stripe W8 (left) and the 20 nm wide stripe W5 (right). The distance D1 between these stripes is given within the image. The step width of each cursor is 7 nm and yields a measurement uncertainty of 10 nm (see 4.4.1.2.)

characteristic	measured values (nm)					mean (nm)
	sample no.	2-13	3-11	5-1	5-18	
D1		4668	4668	4668	4676	**4670**
D2		994[1]	994[1]	997	1001[1]	**996**

Tab. 2: Distances measured in SEM images. The values are taken from Fig. 5 and multiplied by the calibration correction factor 1.0066.
[1] Estimated values beween two cursor positions.

4.4. Calculation of uncertainties

The uncertainties of the certified values were determined by a combination of different approaches:

1. The modeling approach combines all identified uncertainties by their propagation based on a mathematical model according to the procedure described in the GUM [3].

2. Repetition of measurements with the same method covers also sources of uncertainty which are not identified and correspondingly not covered by the modeling approach.

3. The comparison of measurements with different methods (TEM and SEM) covers also unidentified sources of uncertainty which underlay no random variation during the repetition of measurements with only one method.

4.4.1. Sources of uncertainty and their contributions to the combined uncertainty

4.4.1.1. TEM

For TEM measurements the sources of uncertainty are:

1. Tilt of lamella preparation with respect to the plane of layers
2. Tilt of lamella to the TEM axis during measurement
3. TEM adjustment
4. Measurement of lengths on sheet film
5. Calibration of TEM magnification

A maximum tilt of 2° during the preparation of the lamella yields an increase of lengths by less than 0.1%. A tilt of the lamella of 2° to the focal plane of the TEM yields a shortening of all lengths in the image by less than 0.1%. Focusing of TEM with respect to image sharpness causes small variations in magnification and, as a consequence, differences in lengths of 1% in maximum. The standard deviations given in Tab. 1 include the effects 1-3. All these contributions to the uncertainty of length measurement are small compared to the contributions 4 and 5.

All lengths in the TEM images on negative sheet film were measured with different glass scales and a measuring loupe. All scales have 0.1 mm as a smallest division. The non-certified 100 mm glass scale (from Graticules Pyser-SGI LTD.) and the measuring loupe (1983 Scale Loupe from Peak Optics) were checked with a certified 50 mm glass scale (from Leica Microsystems) which gives a tolerance of 0.01 mm for the entire length of 50 mm. The comparison of scales yielded no deviations and therefore the contribution of the measuring

scales to the total measurement uncertainty is negligibly small compared to the contribution of scale-reading accuracy.

Scale-reading accuracy depends on the sharpness of images. At the smallest magnification used (M = 10 000) the images show sharp edges and the accuracy of 0.1 mm corresponds to the smallest division of the glass scales. At higher magnifications the edges of the stripes and the narrow stripes are more diffuse (Fig. 4) and the uncertainty of length measurement on the sheet film u_{LF} increases. In Tab. 3 these uncertainties are given in Columns 5 (mm) and 6 (nm), respectively. Because unidentified sources of uncertainty may influence the results also the double standard deviation determined from repetition measurements (Tab. 1) was taken into account. In Column 8 of Tab. 3 the greater value from either estimation (Col. 6) or repetition (Col. 7) is given as the uncertainty of length measurement on the sheet film.

The magnification of the TEM was calibrated by imaging a calibration standard with the known length $L_{S.}$ According to (1) then the magnification may be calculated by $M = L_F / L_S$, where L_F is the length of the image on sheet film. Therefore the uncertainty of TEM magnification u_M is caused by two sources:

1. The uncertainty u_{LS} of the calibration standard MAG*I*KAL™ is given as 2 %.
2. The uncertainty u_{LF} of the calibration process is 1.6 % which corresponds to the mean deviation of M values from the linear calibration function. These values must be combined according to the law of propagation of uncertainties:

$$\frac{u_M}{M} = \sqrt{\left(\frac{u_{LS}}{L_S}\right)^2 + \left(\frac{u_{LF}}{L_F}\right)^2} = \sqrt{0.02^2 + 0.016^2} \approx 0.026 \qquad (2)$$

which corresponds to a relative uncertainty of 2.6 %. This value may be reduced by taking into account the results of SEM measurements.

The calibration of TEM and SEM instruments was done with different standards and therefore the TEM and REM measurements could be considered as two independent ones. Then the consistency of results for D1 and D2 (see Tabs. 1 and 2) lead to a reduction of the uncertainties of calibration. According to the definition of standard deviation these uncertainties may be reduced by a factor of $1/\sqrt{n}$. Thus, the reduced relative uncertainty of TEM magnification is

$$\frac{u_{Mr}}{M} = \frac{1}{\sqrt{n}} \times \frac{u_M}{M} = \frac{1}{\sqrt{2}} \times 0.026 \approx 0.018 \quad . \qquad (3)$$

4.4.1.2. SEM

The measurement uncertainty of distances measured by SEM and correspondingly the uncertainty of SEM calibration results from two sources:

1. The uncertainty of length measurement u_{LM} due to the positioning of the measuring cursors (Fig. 5). From a step width of 7 nm for each cursor follows from the propagation of uncertainties: $u_{LM} = [(7\ \text{nm})^2 + (7\ \text{nm})^2]^{1/2} \approx 10\ \text{nm}$

2. The length scale of the SEM was calibrated by means of a silicon chip with etched groups of lines (IMS HR 98 727-04 183). The certificate from PTB (calibration mark 4319PTB05) gives an expanded (k=2) uncertainty of 20 nm for all distances between 1 µm and 10 µm.

The combination of both sources of uncertainty according to Equ. (2) gives an uncertainty of SEM calibration of u_{cal} = 22 nm. This corresponds to relative uncertainties of 0.5 % for D1 = 4.67 µm and 2.2 % for D2 = 996 nm, respectively.

4.4.2. Calculation of combined uncertainty

4.4.2.1. TEM

The length L measured by TEM is given by $L = L_F / M$, where L_F is the length measured on sheet film and M is the magnification of TEM taken from the linear calibration curve. Correspondingly the measurement uncertainty u_L follows from the uncertainties of the length measurement on the sheet film u_{LF} and the reduced uncertainty of magnification u_{Mr}

$$\frac{u_L}{L} = \sqrt{\left(\frac{u_{LF}}{L_F}\right)^2 + \left(\frac{u_{Mr}}{M}\right)^2} \quad . \tag{4}$$

The calculation of combined uncertainties for TEM measurements is shown in Tab. 3. According to the strategy for the calculation of uncertainties (see 4.4.) u_{LF} is determined either from an estimation of uncertainties (Column 6) or from repeated measurements (Column 7). The greater value (Column 8) is combined with the reduced uncertainty of magnification and yields the measurement uncertainty of length. All measured values (Tab. 1) are situated within the uncertainty range $L \pm U_L$.

4.4.2.2. SEM

The combined uncertainty of length measured by SEM will be calculated for the distance D1 = 4.67 µm only, because only this value will be certified on the basis of SEM results. The uncertainty of length is $u_L = (u_{LM}^2 + u_{cal}^2)^{1/2} = [(10\ \text{nm})^2 + (22\ \text{nm})^2]^{1/2} \approx 24\ \text{nm}$, where u_{LM} and u_{cal} are taken from 4.4.1.2. With k=2 this value yields an expanded uncertainty U_L= 48 nm.

col. no.	1	2	3	4	5	6	7	8	9	10	11	12
characteristic	certified value from Tab. 1 (nm)	uncertainty of length measurement on sheet film u_{LF}								relative uncertainty of TEM magnif. M (u_{Mr} / M) x 100 %	combined relative uncertainty of Length L (U_L / L) x 100 %	combined absolute uncertainty of Length L U_L (nm)
		estimated uncertainty of length measurement					2 ∗ stand. dev. from Tab. 1 (nm)	greater value from cols. 6 and 7 U_{LF} (nm)	relative uncertainty of L_F (U_{LF} / L_F) x 100 %			
		number of image	real magnific. M x 1000	measured length (mm)	absolute uncertainty (mm)	absolute uncertainty (nm)						
W1	691	7328	9.76	6.75	0.1	10.0	19.9	19.9	2.9	1.8	3.40	**23**
W2	691	7328	9.76	6.75	0.1	10.0	19.9	19.9	2.9	1.8	3.40	**23**
W3	293	7463	29.3	8.5	0.2	7.0	7.0	7.0	2.4	1.8	2.99	**9**
W4	294	7463	29.3	8.5	0.2	7.0	7.4	7.4	2.5	1.8	3.09	**9**
W5	19	7463	29.3	0.6	0.1	1.7	1.6	1.7	8.9	1.8	9.13	**1.7**
W6	195	7463	39.0	7.6	0.2	5.0	3.8	5.0	2.6	1.8	3.13	**6**
W7	195	7465	39.0	7.6	0.2	5.0	3.8	5.0	2.6	1.8	3.13	**6**
W8	38	7845	39.0	1.5	0.1	2.5	1.5	2.5	6.6	1.8	6.82	**2.6**
W9	3.6	7845	39.0	0.15	0.03	0.8	0.5	0.8	22.2	1.8	22.3	**0.8**
W10	14.2	7845	39.0	0.55	0.05	1.3	1.5	1.5	10.6	1.8	10.72	**1.5**
W11	3.5	8104	293	1.0	0.2	0.7	0.7	0.7	20.0	1.8	20.1	**0.7**
W12	96	7850	97.6	9.4	0.2	2.0	1.8	2.0	2.08	1.8	2.75	**2.6**
P1	587	7463	29.3	17.0	0.2	7.0	13.1	13.2	2.2	1.8	2.88	**17**
P2	389	7465	39.0	16.1	0.2	5.0	7.4	7.4	1.9	1.8	2.62	**10**
P3	273	7465	39.0	10.6	0.2	5.0	4.4	5.0	1.8	1.8	2.57	**7.0**
P4	193	7468	97.6	18.6	0.2	2.0	4.0	4.0	2.1	1.8	2.75	**5.3**
P5	136	7469	97.6	13.1	0.2	2.0	5.6	5.6	4.1	1.8	4.49	**6.1**
P6	97	7470	97.6	9.4	0.2	2.0	2.6	2.6	2.68	1.8	3.23	**3.1**
P7	67.5	7470	97.6	6.5	0.2	2.0	2.3	2.2	3.3	1.8	3.72	**2.5**
P8	48.4	7470	97.6	4.6	0.2	2.0	2.4	2.4	5.0	1.8	5.28	**2.6**
P9	76.6	7851	97.6	7.5	0.2	2.0	1.1	2.0	2.6	1.8	3.17	**2.4**
P10	57	7851	97.6	5.6	0.2	2.0	1.4	2.0	3.5	1.8	3.94	**2.2**
P11	42	7851	97.6	4.1	0.1	1.0	0.9	1.0	2.4	1.8	2.98	**1.3**
P12	31	7851	97.6	3.0	0.1	1.0	0.0	1.0	3.2	1.8	3.69	**1.1**
P13	23	7850	97.6	2.1	0.1	1.0	1.0	1.0	4.3	1.8	4.69	**1.1**
P14	17.5	7850	97.6	1.7	0.1	1.0	1.0	1.0	5.7	1.8	5.99	**1.0**
P15	13.3	8437	293	4.0	0.3	1.0	1.1	1.1	8.3	1.8	8.46	**1.1**
P16	9.4	8437	293	2.8	0.3	1.0	1.4	1.4	14.9	1.8	15.00	**1.4**
P17	6.9	8437	293	2.0	0.3	1.0	0.6	1.0	14.5	1.8	14.60	**1.0**
D1	4642	7471	14.6	67.5	0.2	14.0	28.0	28.0	0.6	1.8	1.90	**88**
D2	986	7845	39.0	38.6	0.2	5.0	12.9	12.9	1.3	1.8	2.23	**22**
D3	492	7845	39.0	19.3	0.2	5.0	7.0	7.0	1.4	1.8	2.29	**11.3**
D4	1264	7846	39.0	49.4	0.2	5.0	10.3	10.3	0.8	1.8	1.98	**25**
D5	237	7850	97.6	23.2	0.2	2.0	7.1	7.1	3.0	1.8	3.49	**8.3**
D6	114	8104	293	33.4	0.3	1.0	1.9	1.9	1.7	1.8	2.45	**2.8**

Tab. 3: Calculation for the uncertainty of lengths measured by TEM. All images given in col. 2 are shown in Fig. 4. The calculation of u_L/L in col. 11 was carried out by using Equ. (4).

Characteristic	Certified Value (nm)	Expanded (k=2) Uncertainty (nm)
W1	691	23
W2	691	23
W3	293	9
W4	294	9
W5	19.5	1.7
W6	195	6
W7	195	6
W8	38	2.6
W9	3.6	0.8
W10	14.2	1.5
W11	3.5	0.7
W12	96	2.6
P1	587	17
P2	389	10
P3	273	7
P4	193	5
P5	136	6
P6	97	3
P7	67.5	2.5
P8	48.5	2.6
P9	76.5	2.4
P10	57	2.2
P11	42	1.3
P12	31	1.1
P13	23	1.1
P14	17.5	1.0
P15	13.3	1.1
P16	9.4	1.4
P17	6.9	1.0
D1	4670*	48*
D2	986	22
D3	492	11.3
D4	1264	25
D5	237	8.3
D6	114	2.8

*Tab. 4: Certified values (for definition see Fig. 3) and their uncertainties (from Tab. 3). Values are taken from TEM images, * D1 is taken from SEM images. W – stripe width, P – period of a square-wave grating, D – center to center distance between stripes or between stripes and gratings, respectively.*

characteristic	non-certified value (nm)
W13	*5*
W14	*1*
P0	*147 (80 AlGaAs + 67 GaAs)*
P18	*4.6*
P19	*3*
P20	*2*
P21	*23 (5 InGaAs + 18 GaAs)*
P22	*15 (5 InGaAs + 10 GaAs)*
P23	*10 (5 InGaAs + 5 GaAs)*

Tab. 5: Non-certified values, for information only. For definition see Fig. 3.

5. Homogeneity of samples

It is necessary to ensure that certified values are valid for all samples made from a batch of wafers coated during one MOVPE procedure. But certification measurements were made on a limited number of samples only. Therefore two assumptions have to be fulfilled:

1. The layer thickness is approximately constant over the area where the samples are taken from and

2. there is no difference in layer thickness between the 5 wafers coated during one MOVPE procedure (batch homogeneity).

The validity of these assumptions will be evaluated in the next sections.

5.1. Homogeneity of layer thickness across the wafer

The layers were grown by MOVPE on 4" GaAs wafers. Rotation of the substrate carrier during the layer growth ensures excellent deposition homogeneity regarding layer thickness and composition. Therefore the thickness of layers is expected to be isotropic (see 5.1.2.). Slightly different temperature conditions between central and outer regions of the wafer may cause small variations in layer thickness. The analysis of this radial variation of layer thickness and as a consequence the definition of the usable wafer area are the goal of the following investigations.

5.1.1. High Resolution X-ray Diffraction

Measurements of High Resolution X-ray Diffraction (HRXRD) were made at the "Ferdinand-Braun-Institut für Höchstfrequenztechnik", the manufacturer of the layer system. For the examination of layer thickness and its homogeneity a Distributed Bragg Reflector (DBR, Tab. 6) with 12 periods was placed at the top of the multilayer system (Fig. 1.). The analysis of a DBR layer stack with HRXRD gives a pattern of sharp diffraction peaks (rocking curve) which is very sensitive to the variation of the layer thickness. In a first step a test structure consisting only of the DBR layer stack was grown. In contrast to the very complex multilayer system of BAM-L200 the rocking curve of this simple system can be calculated by simulation (Fig. 6).

Number of layers	material	layer thickness (nm)
1	GaAs	100
12	$Al_{0.7}Ga_{0.3}As$	80
12	GaAs	67

Tab. 6: Parameters of the Distributed Bragg Reflector

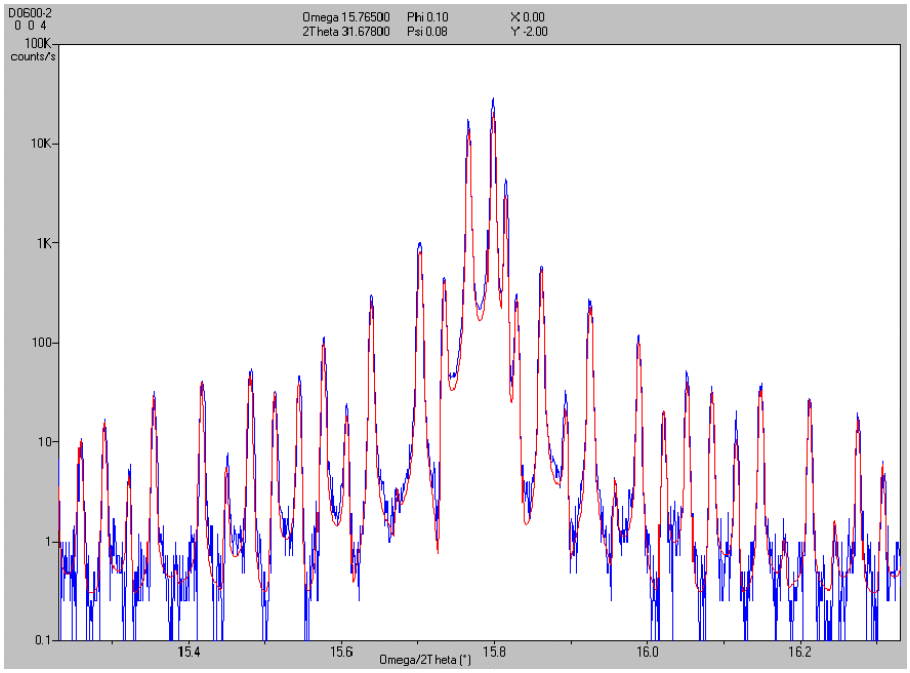

Fig. 6: Measured (blue) and simulated (red) rocking curve of the DBR test structure

To analyze the radial variation of layer thickness HRXRD measurements were made at the center and 40 mm from the center (= 10 mm from the edge) of the wafer (Fig. 7). Fitting these curves a variation of thickness below 1% was found (Tab. 7).

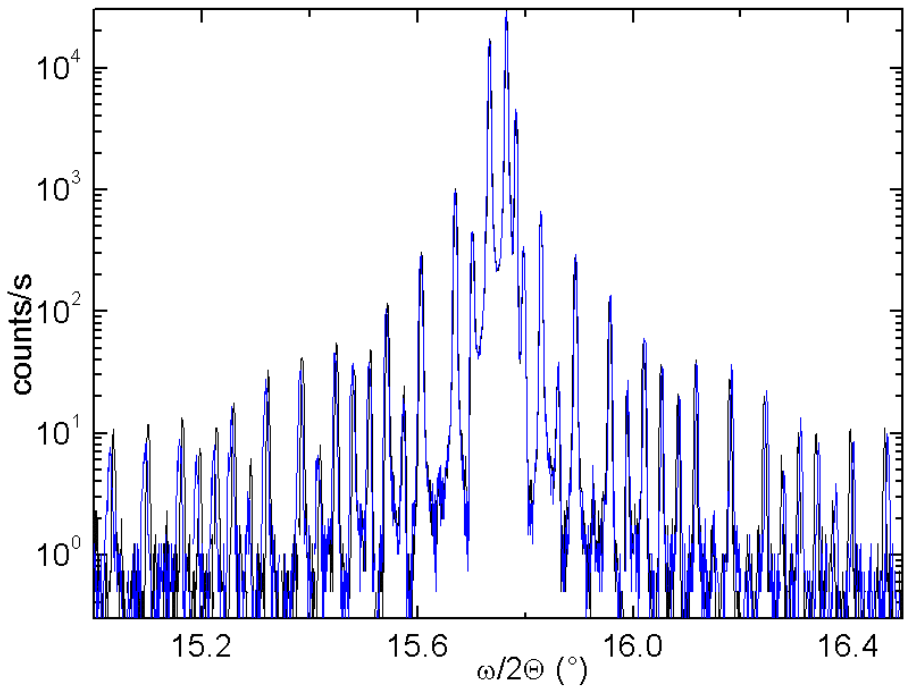

Fig. 7: Rocking curves of the DBR test structure measured at the center (black) and 40 mm from the center (blue) of the wafer.

Parameter	center	40 mm from center	rel. difference (%)
x ($Al_xGa_{(1-x)}$ As)	0.7	0.7	0
d ($Al_xGa_{(1-x)}$ As) (nm)	80.6	79.9	-0.9
d (GaAs) (nm)	63.6	63.1	-0.8
period (nm)	144.2	143.0	-0.8

Tab. 7: Difference of layer thickness d from central to outer region of the wafer determined by fitting the HRXRD measurements shown in Fig. 7.

The fitting procedure is demonstrated by simulated curves (Fig. 8). Variations of ± 1.8 nm (1.3 %) in layer thickness (and therewith DBR period) yield a measurable difference in the distance between neighboring diffraction peaks Δ(ω/2θ) and confirms the sensitivity of the method in detecting small variations of the layer thickness.

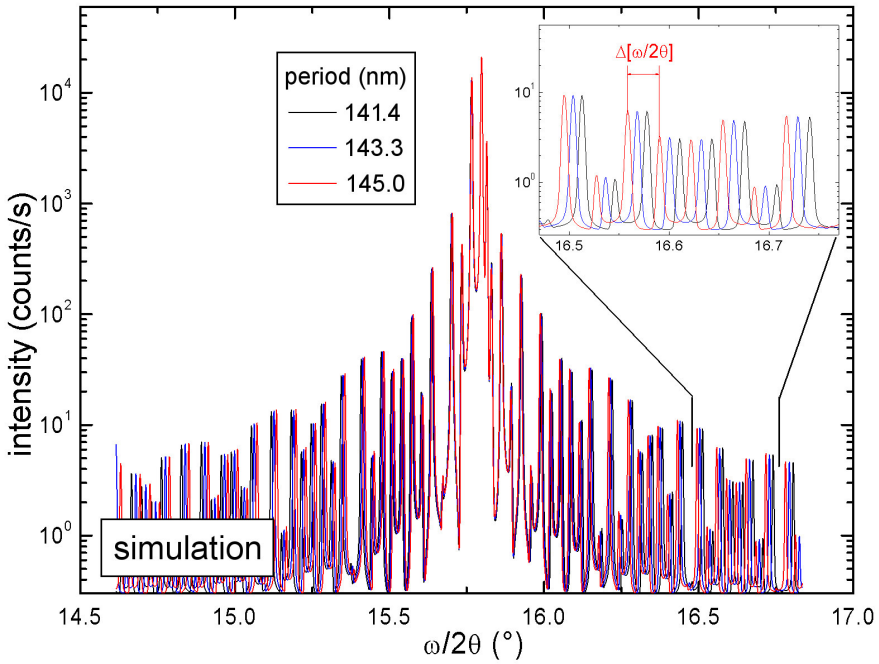

Fig. 8: Simulated rocking curves for a DBR structure with different periods. The distance between neighboring diffraction peaks Δ(ω/2θ) is visible in the insert.

The analysis of the test structure has shown that

1. HRXRD measurements are suitable for the detection of small variations in layer thickness and

2. The variation of the layer thickness between the center of the wafer and the outer region (r = 40 mm) is about 1 %.

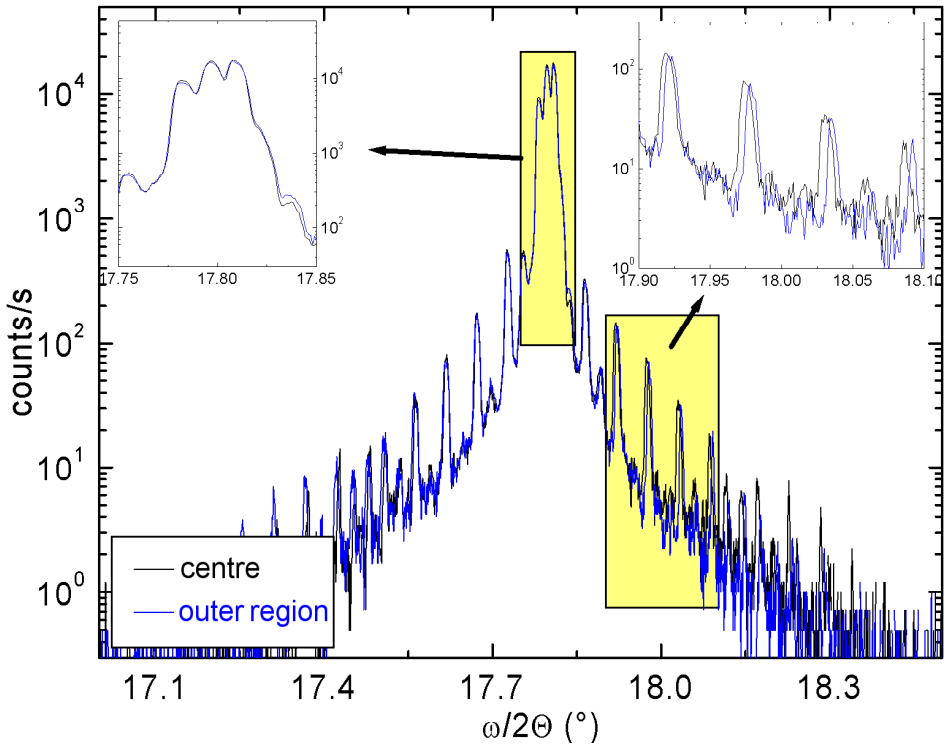

Fig. 9: *Rocking curves of the BAM-L200 layer stack measured at the center (black) and 40 mm from the center (blue) of the wafer.*

The layer system of BAM-L200 is too complex for a simulation of rocking curves. Therefore no quantitative analysis of variations in layer thickness is possible. But the very small difference between rocking curves measured in the central and outer regions of the wafer (Fig. 9) confirms a high homogeneity of the layer thickness. Furthermore the growing conditions were the same as used for the test structure and therefore the variation in layer thickness measured at the test structure (about 1 %) may also be valid for the BAM-L200 layer stack.

5.1.2. Optical reflection spectroscopy

Measurements of optical reflection spectra were made at the “Ferdinand-Braun-Institut für Höchstfrequenztechnik”, the manufacturer of the layer system. In contrast to the time consuming HRXRD measurements this method is fast and enables scanning of the whole wafer. Simulation of the reflection spectrum shows that the position of the stop band (reflectivity close to 1) is very sensitive to the variation of layer thickness (Fig. 10). The relation between stop band position and DBR period gives a linear calibration function (Fig. 11) and enables the use of stop band position as a measure of the layer thickness.

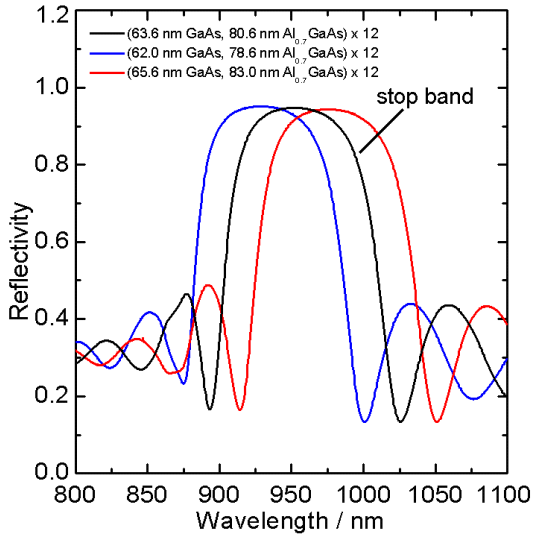

Fig. 10: Simulated reflection spectra for different grating periods

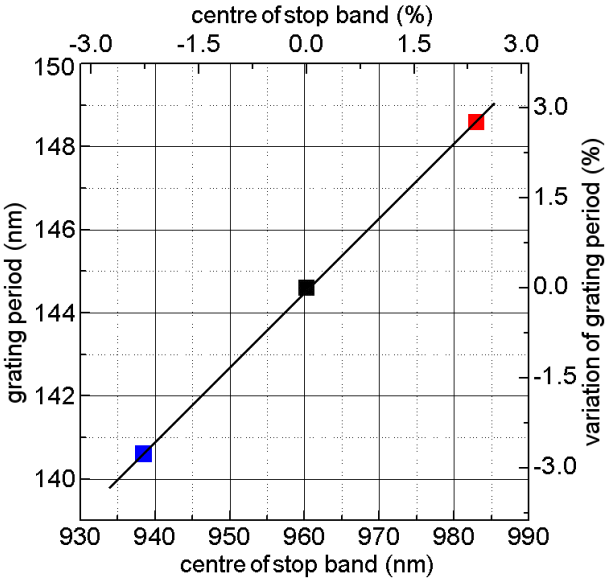

Fig. 11: Relation between grating period and center of stop band. The values are taken from Fig. 10.

Fig. 12 shows the measured and calculated reflection spectra for the DBR test structure (parameters in Tab. 4). The layer thicknesses determined by fitting the measured curve (63.8 nm and 80.8 nm) are very close to the values determined by HRXRD (63.6 nm and 80.86 nm, Tab. 5). This agreement of values supports the accuracy of both methods.

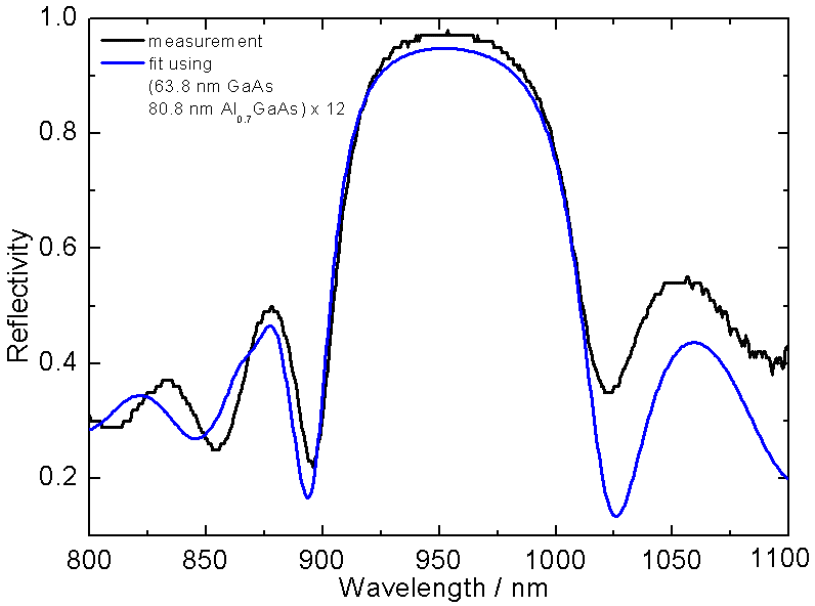

Fig.12: Measured (black) and calculated (blue) reflection spectrum of the DBR test structure

Fig. 13a shows a map of stop band position measured over the whole area of the wafer. The variation of stop bands is nearly isotropic. A line profile through the map (Fig. 13b) shows 11 nm and 5 nm shifts of stop band position between the center and the ± 40 mm and ± 30mm positions, respectively. According to the calibration curve (Fig. 11) these stop band shifts correspond to variations of grating periods of 2 nm (1.4 %) and 1 nm (0.7 %).

The layer system of BAM-L200 is too complex for a simulation of reflection curves. Therefore no calculation of period variations from the stop band position is possible. Fig 14 shows that the stop band position is shifted by 12.5 nm and 6 nm, respectively. These values are similar to those measured for the DBR test structure (Fig. 13b) and therefore the variation of thickness could be estimated to about 1.5 % also.

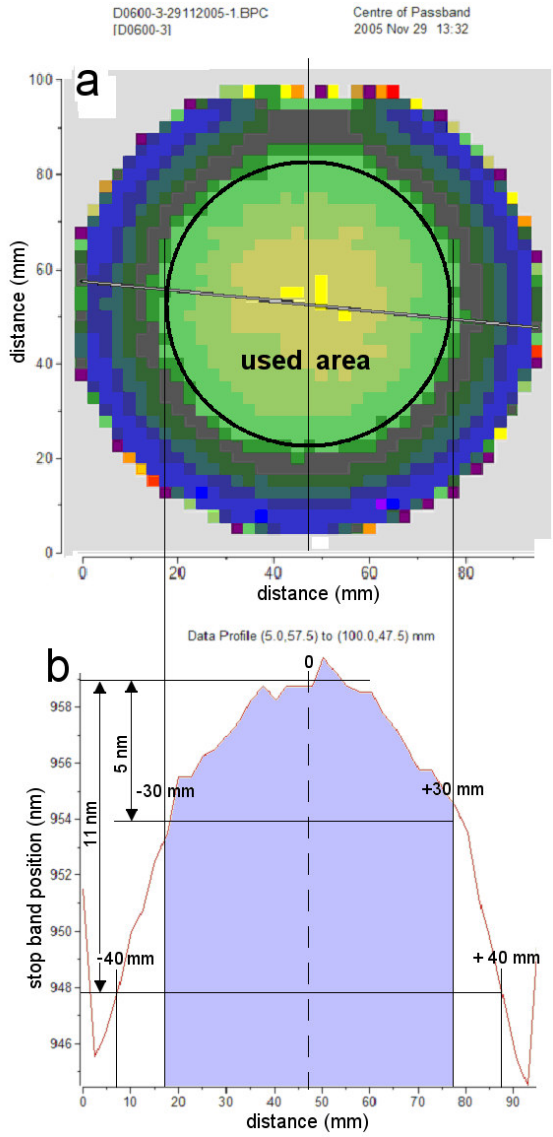

Fig. 13: Map (a) and line profile (b) of stop band position measured at the DBR test structure. The black circle in (a) marks the used area of the wafer.

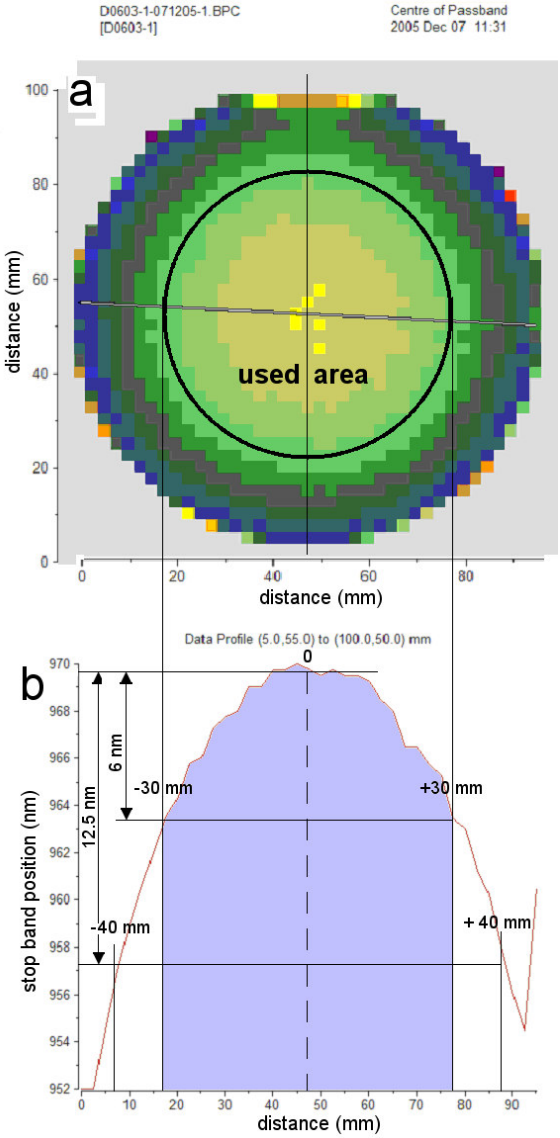

Fig. 14: Map (a) and line profile (b) of stop band position measured at the BAM-L200 layer stack.

5.1.3. TEM measurements

In Tab. 1 no significant difference in layer thicknesses between the positions 5 mm and 30 mm is visible. To find the limit of the useful area we measured two TEM-lamellae taken 40 mm from the center of the wafer. Tab. 8 shows selected characteristics measured at these lamellae. The measured lengths (except for D6) are significantly smaller than those measured at 5 mm and 30 mm from the center, respectively, and most of the values were outside the uncertainty range of the certified value.

characteristic	certified value 5 mm - 30 mm (nm)	measured values 40 mm (nm)			mean 40 mm (nm)	deviation from cert. value %
W1	691 ± 23	656			**656**	**-5.1**
W12	96 ± 2.6	92			**92**	**-4.2**
P1	587 ± 17	563			**563**	**-4.1**
P2	389 ± 10	374			**374**	**-3.9**
D1	4642 ± 24	4431			**4431**	**-4.5**
D2	986 ± 22	967	962	969	**966**	**-2.0**
D5	237 ± 8.3	231	233	236	**233**	**-1.5**
D6	114 ± 2.8	113	115	113	**113.7**	**-0.3**

Tab. 8: Values measured 40 mm from the center of the wafer and their deviations from the certified values. The numbers of sheet films in which the lengths were measured are given in Tab. A2 (appendix).

5.1.4. Definition of used area

Measurements of optical reflection spectra show an isotropic decrease of layer thicknesses from the center to the edge of the wafer (Figs. 13 and 14). TEM measurements show that this decrease is not significant at 30 mm from the center but becomes significant 40 mm from the center (Tabs. 1 and 8).

As a consequence we decided to use only the area within a radius of 30 mm (see Figs. 13 and 14) of the 4-inch wafers (r = 50 mm) for the preparation of the certified reference material BAM-L200.

5.2. Wafer-to-wafer homogeneity

A batch of 5 wafers was coated during one MOVPE process. The wafer-to-wafer homogeneity of two wafers was tested by SEM measurements. The samples 2-13, 3-11 and 3-12 were taken from wafer D0603-2 and the samples 5-1 and 5-18 were taken from wafer D0603-1, respectively. Fig. 5 and Tab. 2 show no significant differences between the samples taken from different wafers. Therefore, the expected wafer-to-wafer homogeneity is confirmed.

6. Stability of samples

$AlxGa_{1-x}As$ - GaAs – multilayers are long-term stable systems. However, oxidation of the $Al_{0.7}Ga_{0.3}As$ leads to height differences of 2 – 4 nm between $Al_{0.7}Ga_{0.3}As$ and GaAs stripes in the surface. These small height differences do not influence the imaging. The formation of oxide layers during storage on air cannot be avoided. Sputtering can be an appropriate procedure to remove them. Ion beams used for sputter cleaning or as a probe may result in changes of surface topography. This effect has to be considered by the user.

A sample which is a cross section of a layer stack has the same lateral element distribution over the whole depth. Therefore it is possible to renew the sample surface by careful grinding and polishing.

7. Fields of Application

BAM-L200 can be used by all methods of surface analysis which are sensitive to a material contrast between $Al_{0.7}Ga_{0.3}As$ and GaAs. Successful tests have been accomplished with Secondary Ion Mass Spectrometry (Fig. 15), Auger Electron Spectroscopy (Fig. 16), Energy Dispersive X-ray Spectrometry and Electron Spectroscopy for Chemical Analysis (NanoESCA endstation at a synchrotron radiation source).

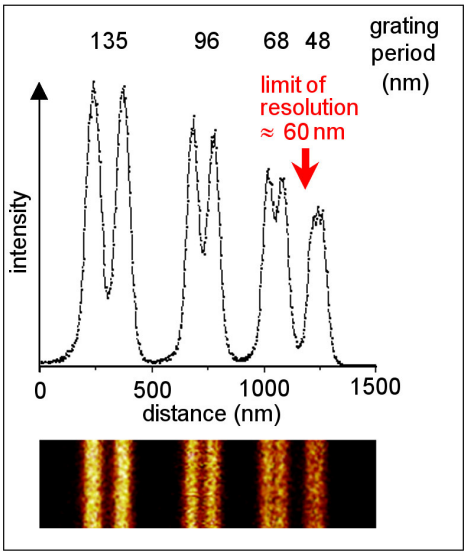

Fig. 15: Al image and profile measured by SIMS. Data courtesy of ION-TOF GmbH, Münster, Germany

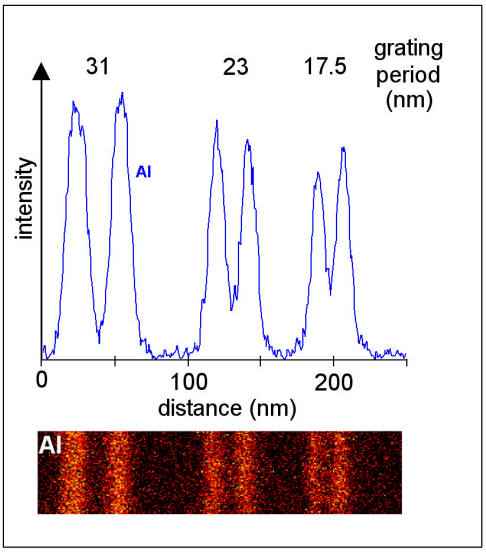

Fig. 16: Al image and profile measured by AES. Data courtesy of Physical Electronics, Inc., USA

Imaging of the sample allows the real time estimation of lateral resolution: The period of the smallest resolved square-wave grating corresponds to the lateral resolution of the image (see Fig. 15).

Numerical analysis of the image of square-wave gratings of different periods enables the determination of the modulation transfer function (MTF). Furthermore narrow stripes between 1 nm and 40 nm enable the determination of the line spread function (LSF) and step transitions enable the determination of the edge spread function (ESF). All these functions describe the lateral resolution of the image.

Certified distances D may be used for the calibration of length scales. The certified values are center-to-center distances between narrow stripes and/or fine 3-stripe gratings, respectively. This definition of distance does not depend on lateral resolution, because the center of a stripe or a grating (resolved or not resolved) does not vary with resolution.

8. Instructions for users

A delivered sample was cleaned with a rinsing agent and flushed with distilled water to remove particles from polishing. Despite this procedure, there may be, however, some particles remaining on its surface. Areas affected by those particles should not be used for imaging. Contaminations may be removed from the surface by wet cleaning or sputtering, but sputtering may change the surface topography.

The full metal packaging of the semiconductor platelet ensures the conductivity of the whole sample. The sample is suitable for ultra high vacuum applications.

9. References

Guidelines for the Development of BAM Reference Materials, Berlin, 2006, www.bam.de

Reference materials – General and statistical principles for certification, ISO Guide 35: 2006

[1] M. Senoner, W. E. S. Unger, Lateral resolution of Secondary Ion Mass Spectrometry - results of an inter-laboratory comparison, Surface and Interface Analysis 39 (2007), 16-25

[2] M. Senoner, Th. Wirth, W. Unger, W. Österle, I. Kaiander, R. L. Sellin and D. Bimberg, BAM-L002 - A new type of certified reference material for length calibration and testing of lateral resolution in the nanometre range, Surface and Interface Analysis 36 (2004), 1423-1426

[3] Guide to the expression of uncertainty in measurement (GUM), ISO/IEC Guide 98:1995

Appendix

characteristic	measured values (nm)																					
	5 mm														30 mm							
W1	**692**	7328					**676**	8116	**697**	7472					**697**	7926						
W2	**692**	7328					**676**	8116	**697**	7472					**697**	7926						
W3	**297**	7328	**290**	7330	**297**	7408	**290**	8116	**292**	7472	**290**	7463			**297**	7926						
W4	**297**	7328	**290**	7330	**297**	7408	**290**	8116	**297**	7472	**290**	7463			**297**	7926						
W5			**19**	7330	**19**	7408					**19**	7463	**20.5**	7471								
W6	**195**	7328	**191**	7330	**195**	7408	**196**	7409	**195**	7465	**195**	7463	**198**	7471	**195**	7926						
W7	**195**	7328	**191**	7330	**195**	7408	**196**	7409	**195**	7465	**195**	7463	**198**	7471	**195**	7926						
W8	**38.5**	7853	**38.5**	7844	**37**	7417	**38.5**	7845	**37**	7473							**38.5**	8107				
W9	**3.8**	7853	**3.6**	7844			**3.8**	7845									**3.3**	8107				
W10	**15**	7853	**15**	7844	**14**	7417	**14**	7845	**14**	7473							**13**	8107				
W11	**4**	7850	**3.4**	7863							**3.4**	8426					**3.4**	8104	**3.1**	8099		
W12	**96**	7850	**95**	7848	**97.5**	7846			**96**	7480			**96**	8456			**95**	8114				
P1	**594**	7328	**580**	7330	**590**	7408	**580**	8116	**589**	7472	**580**	7463			**594**	7926						
P2	**394**	7328	**382**	7330	**392**	7408	**392**	7409	**387**	7465	**389**	7463	**390**	7471	**389**	7926						
P3	**277**	7328					**272**	7409	**272**	7465			**274**	7471	**272**	7926						
P4	**195**	7328			**192**	7413	**192**	7409	**191**	7468	**196**	8212	**192**	7471	**195**	7926						
P5	**133**	7411					**137**	8212	**134**	7469	**140**	7866	**137**	7471	**133**	7926						
P6	**95**	7411	**96**	7412	**97**	7416	**99**	8212	**96**	7470	**98**	8208	**96**	7471	**97**	7926						
P7			**67.5**	7412	**68.5**	7416	**68**	8212	**67**	7470	**65.5**	8208	**68.5**	7471								
P8			**49**	7412	**48**	7416	**50.5**	8212	**47**	7470	**48**	8208	**48**	7471								
P9	**77**	7851							**77**	7478	**76**	8454			**77**	8098	**76**	8114				
P10	**57**	7851							**58**	7478	**57**	8454			**57**	8098	**56**	8114				
P11	**42**	7851							**42**	7478	**42**	8454			**43**	8097	**42**	8114				
P12	**31**	7851	**31**	7850	**31**	7848					**31**	8454	**31**	8456	**31**	8097	**31**	8114				
P13	**22.5**	7851	**22.5**	7850	**22.5**	7848					**23.5**	8454	**22.5**	8456	**23.1**	8097	**23.6**	8114				
P14	**17.5**	7851	**16.9**	7850	**17.4**	7848							**17.5**	8456	**17.1**	8097	**18.4**	8114				
P15	**13.0**	7863	**12.3**	7850							**13.7**	8437	**13.7**	8426	**12.8**	8097	**13.3**	8114	**13.7**	8099	**13.7**	8104
P16	**9.5**	7863	**8.2**	7850							**9.5**	8437	**10.2**	8426	**8.5**	8097	**9.2**	8114	**10.2**	8099	**9.5**	8104
P17	**7.5**	7863									**6.8**	8437	**6.8**	8426					**6.8**	8099	**6.8**	8104
D1	**4641**	7329	**4662**	7333	**4652**	8118	**4623**	7471							**4631**	7926	**4641**	7927				
D2	**990**	7845	**989**	7333	**977**	7417	**973**	7473	**986**	7866			**982**	8458	**994**	7926	**989**	7927	**987**	8103	**989**	8110
D3	**496**	7845			**488**	7417	**486**	7473	**493**	7866			**490**	8458	**492**	7926	**492**	7927	**492**	8103	**497**	8110
D4	**1269**	7852	**1265**	7846	**1270**	8118			**1264**	7866	**1255**	8452					**1260**	7927			**1263**	8110
D5	**238**	7850	**241**	7846					**238**	7848	**233**	8456	**240**	8426					**232**	8097	**234**	8114
D6	**115**	7850	**115**	7863					**114**	7848	**113**	8456	**116**	8426	**114**	8104	**114**	8099	**114**	8097	**113**	8114

Tab. A1: The bold numbers are the measured lengths given in Tab. 1. The four digit numbers after the lengths are the image numbers of the corresponding sheet films in the division AC of the image archive of BAM department V.11.

Appendix

characteristic	measured values (nm) 40 mm					
W1	**656**	7486				
W12	**92.0**	7751				
P1	**563**	7486				
P2	**374**	7486				
D1	**4431**	7486				
D2	**967**	7482	**962**	7483	**969**	7761
D5	**231**	7487	**233**	7751	**236**	7750
D6	**113**	7488	**115**	7751	**113**	7750

Tab. A2: The bold numbers are the measured lengths given in Tab. 8. The four digit numbers after the lengths are the image numbers of the corresponding sheet films in the division AC of the image archive of BAM department V.11.